Associated production of selectron neutralino pairs

M. Corradi[a]
[a] Universitá di Bologna and INFN Bologna, Via Irnerio 46, Bologna, Italy

Abstract: A Monte Carlo study of the process $ep \to \tilde{e}\chi_1^0 X$ has been performed, including detector simulation and background estimate. Exclusion plots in the $m_{\chi_1^0}$ versus $m_{\tilde{e}}$ plane are provided for different values of integrated luminosity.

1 Introduction

Most of SUSY GUT models predict squarks heavier than sleptons. No-scale supergravity models [1], (that have been the object of renewed interest [2]), predict a ratio $m_{\tilde{q}}/m_{\tilde{e}_R} \gtrsim 3$. In these models, the process $ep \to \tilde{e}\tilde{q}$ has a small cross section or is beyond the accessible region of HERA, given the exisiting LEP1 (sleptons) and TEVATRON (squarks) lower mass bounds. Therefore the associated production of slepton gaugino pairs becomes the most important process for the production of (R_p conserving) SUSY particles [3, 4]

$$e^{\pm}p \to \tilde{e}^{\pm}\chi_i^0, X \tag{1}$$

$$e^{\pm}p \to \tilde{\nu}\chi_i^{\pm}X. \tag{2}$$

Assuming that χ_1^0 is the LSP and that the selectron decays to $\chi_1^0 e$, the signature for process

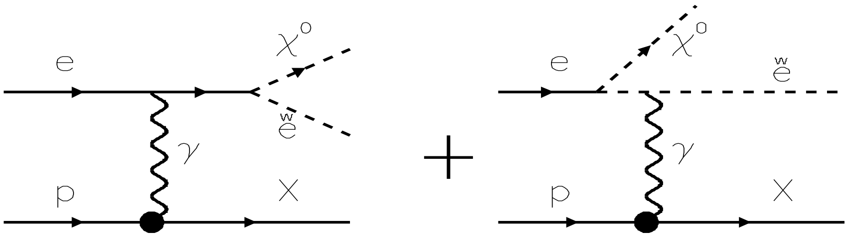

Figure 1: *Relevant graphs for selectron neutralino production.*

(1) is an electron (from selectron decay) and missing P_t (from the two neutralinos). Moreover, the fact that a very low mass neutralino is not yet excluded by other experiments (at least for low $\tan\beta$) makes this channel interesting at HERA. Process (2) may have an higher cross section for some set of SUSY parameters, but it produces various final states, due to different chargino and sneutrino decay channels, some of them leading to jets and missing p_t, not easy to distinguish from Standard Model backgrounds. Only the selectron neutralino production channel (1) is considered in this note.

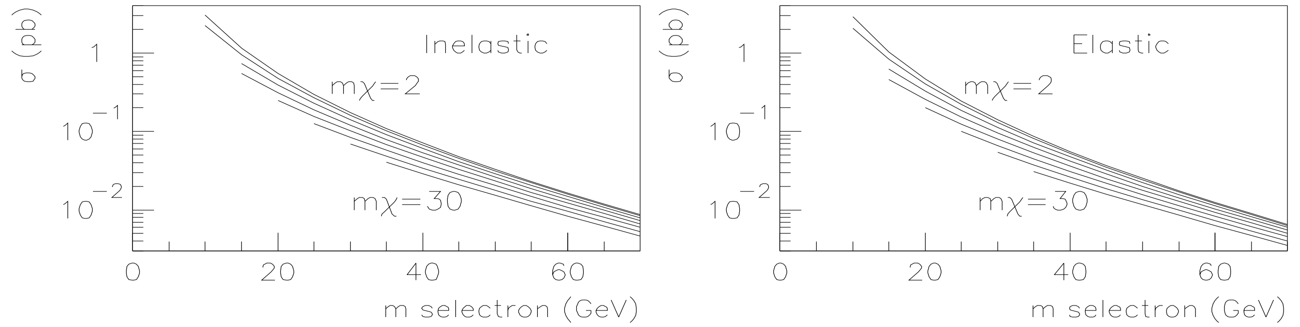

Figure 2: *$ep \to \tilde{e}\chi_1^0 X$ cross section for the elastic and inelastic process as a function of selectron mass in the pure photino limit. Each curve is for a different value of the $m_{\chi_1^0}$ in 4 GeV steps.*

2 Production Cross Section and MC Generator

The relevant Feynman diagrams for process (1) are shown in fig.1. The pair of SUSY particles is produced at the electron vertex. The hadronic final state X can be an elastically scattered proton or an higher mass system.

A monte carlo generator (PYSUS [1]) has been used to evaluate the cross section and to generate events. It is based on a cross section factorized into a photon flux times a parton cross section: $\sigma_{ep\to\tilde{e}\chi_1^0} = \int_{z_{min}}^1 dz f_{\gamma/p}(z)\sigma_{\gamma e\to\tilde{e}\chi_i^0}(sz)$ [4, 5, 6]. The parton ($e\gamma \to \tilde{e}\chi_1^0$) cross section is taken from [4]. In the elastic case, the modified Weizsäcker-Williams approximation [7] is used for the photon flux. In the inelastic case, the photon flux is convoluted from GRV92 parton densities: $f_{\gamma/p}(z) = \sum_i \int_{x_{min}}^1 dx/x \int_{Q^2_{min}}^{Q^2_{max}} dQ^2/Q^2 f_{\gamma/q}(z/x) q_i(x,Q^2)$. The Q^2_{min} cutoff is set to 1 GeV^2, in order to reproduce the inelastic cross section given in ref [6]. Figure 1 shows the cross

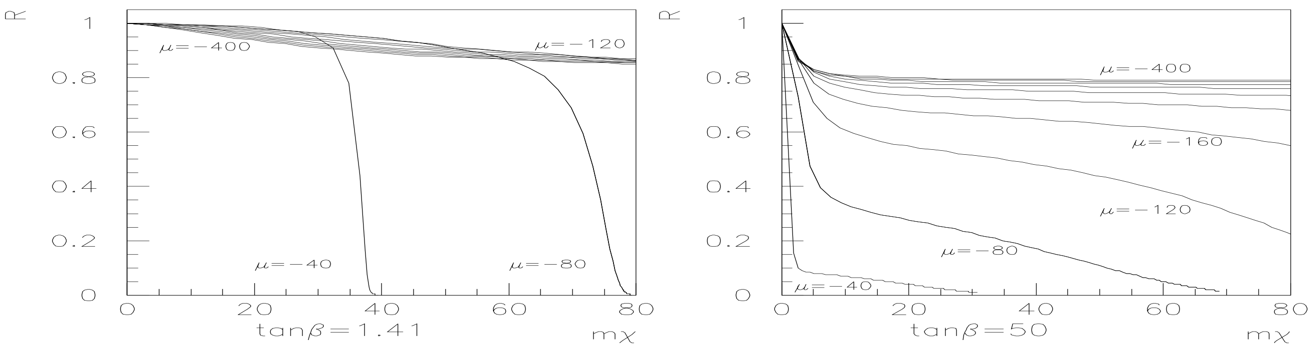

Figure 3: *Ratio of the selectron neutralino to the pure photino cross section (fig. 1) for* $\tan\beta = 1.41$ *(left) and* $\tan\beta = 50$ *(right), as a function of the χ_1^0 mass. The lines are from $\mu = -400$ to $\mu = -40$ in steps of 40.*

section for (left) inelastic and (right) elastic process, as a function of the selectron and neutralino mass. In this plot, the right and left handed selectron are assumed to be mass degenerate and the neutralino to be a pure photino ($\tilde{\gamma}$). Since the value of the $e\chi_1^0\tilde{e}$ coupling constant depends on the neutralino mixing matrix, in the MSSM the total cross section is a function of the parameters $\tan\beta$, μ and M_1. The dependence on these parameters can be included in the normalization factor $R(\mu, \tan\beta, m_{\chi_1^0}) = \sigma_{\tilde{e}\chi_1^0}(m_{\tilde{e}}, m_{\chi_1^0}, \tan\beta, \mu)/\sigma_{\tilde{e}\tilde{\gamma}}(m_{\tilde{e}}, m_{\tilde{\gamma}})$ shown in fig. 3. R is close to 1 in the gaugino region ($|\mu| >> M_1$).

[1]Contact the author for the code and documentation on PYSUS MC generator: `corradi@vxdesy.desy.de`

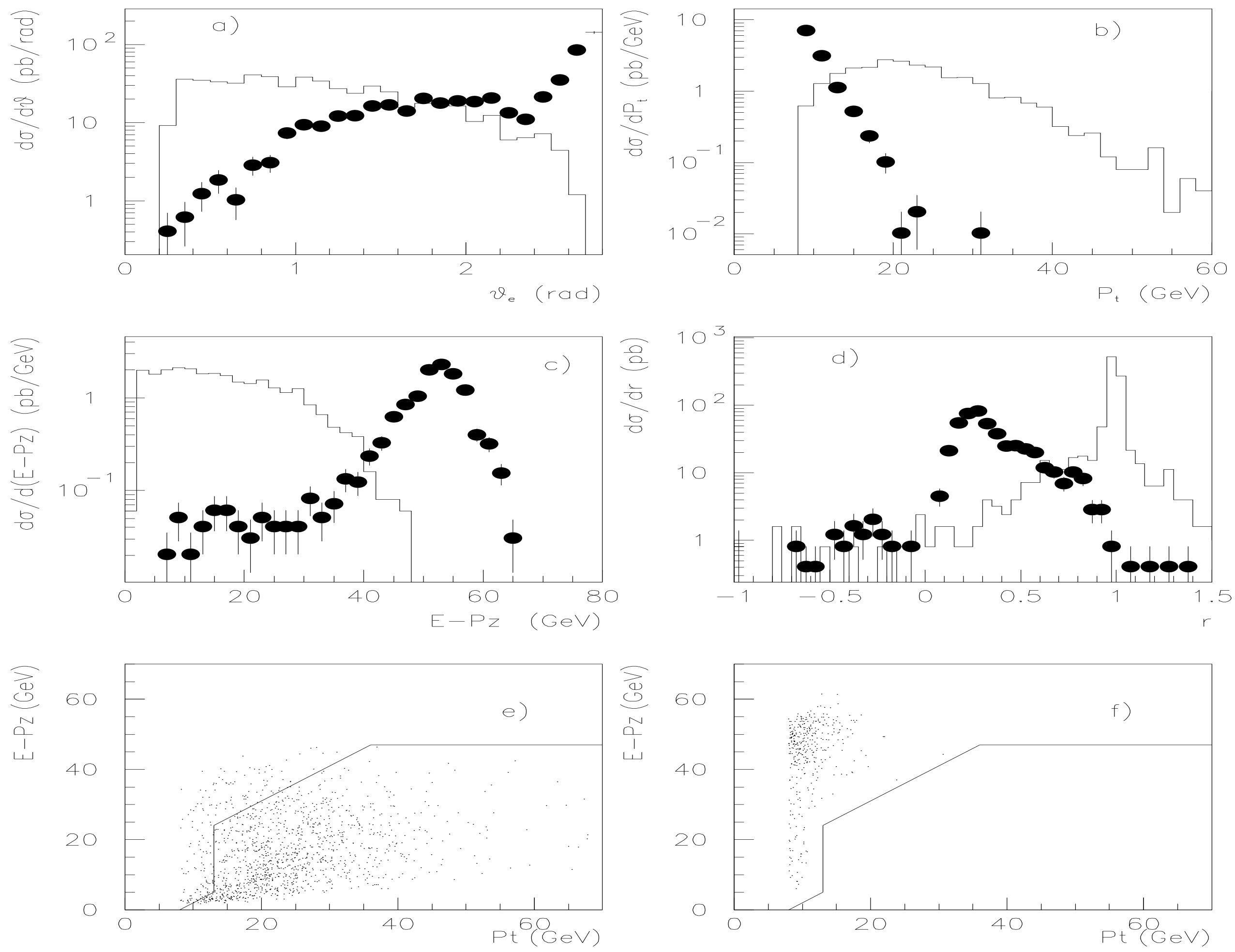

Figure 4: *Detector level distributions for SM background (dots) and for SUSY events ($m_{\tilde{e}} = 40$, $m_{\chi_1^0} = 5$) (line) with arbitrary normalization: a) electron polar angle after cuts 1-3; b) missing P_t, c) $E - P_z$ and d) $r = \mathbf{p}_t^e \cdot \mathbf{p}_t / |p_t|^2$ after cuts 1-4; e) distribution in the $E - P_z$ versus missing P_t plane for SUSY and f) for 48.8 pb^{-1} of NC DIS after cuts 1-5. The line shows the cut adopted in the inelastic selection.*

3 Selection Efficiency and Backgrounds

MC samples of $ep \to \tilde{e}\chi_1^0 X$ and SM backgrounds have been produced and passed through the ZEUS detector simulation. A selection procedure based on the following requests was adopted (see fig. 4 a-d):

1) An isolated electromagnetic cluster in the calorimeter identified as an electron and matching a track of the correct charge from the central tracking detector;

2) missing transverse momentum $P_t > 8$ GeV;

3) standard cuts to remove cosmic muons and beam-gas interactions;

4) polar angle of the electron $\theta_{el} < 2.5 rad$;

5) A cut on the variable $r = \mathbf{p}_t \cdot \mathbf{p}_t^{el} / |\mathbf{p}_t|^2 > 0.4$ (where -$\mathbf{p}_t$ is the missing P_t vector and $\mathbf{p}_t^{el}$ is the electron transverse momentum vector) (fig. 4 d).

$m_{\tilde{e}}$ (GeV)	m_χ (GeV)	Elastic process		Inelstic process	
		a) ϵ (%)	b) ϵ (%)	a) ϵ (%)	b) ϵ (%)
20	5	16	42	16	8
40	5	55	71	44	15
40	25	31	55	28	13
40	35	1	5	2	2
60	5	59	66	51	17
60	25	59	65	51	20

Table 1: *Efficiencies for elastic and inelastic process. a) inelastic selection, b) elastic selection. Obtained from selectron neutralino MC samples of 1000 events each.*

At this point two different selections are made:
a) The inelastic selection, based on a cut in the missing P_t vs $E-P_z$ plane along the line shown in fig. 4 e-f.
b) The elastic selection, obtained by the request of no energy deposit in the calorimeter other than the electron.

Table 1 shows the selection efficiency ϵ for different MC samples. The efficiency depends on the electron p_t spectrum, and therefore on $\Delta m = m_{\tilde{e}} - m_{\chi_1^0}$.

Process	MC Generator	Lumi (pb^{-1})	Inelastic b (fb)	Elastic b (fb)
NC DIS	Herwig, Lepto, Ariadne $Q^2 > 100$	48.8	0	0
CC DIS	Lepto $Q^2 > 100$	490	0	0
$c\bar{c}$	Pythia $P_t^{miss} > 8$	50	0	0
$b\bar{b}$	Pythia $P_t^{miss} > 8$	64	0	0
$\gamma\gamma$ elast.	Lpair $P_t^e > 5$	1910	0	0.5
$\gamma\gamma$ inelast.	Lpair $P_t^e > 5$	782	0	1.3
W^+ DIS	Epvec	10000	17.9	0
W^+ resolved	Epvec	10000	12.3	1.0
Z0 DIS	Epvec	14300	1.5	.07
Z0 quasi-elast.	Epvec	27000	1.3	0
Z0 resolved	Epvec	15600	0	0
Z0 elastic	Epvec	20000	2.4	2.8
TOTAL			35.4	5.7

Table 2: *SM backgrounds. The table shows the process, the MC generator and the generator level cuts, the MC luminosity used and the background rate (i.e. the number of surviving events normalized to 1000 pb^{-1}) for the inelastic and elastic selection.*

The following background processes have been considered: NC DIS, CC DIS, heavy quark production, $\gamma\gamma$ interaction and vector boson production. The MC equivalent luminosity and the rate of surviving events b are given in table 2. The inelastic selection is affected by an high background from W production ($ep \to WeX$, $W \to e\nu$, with the scattered electron undetected). The background for the elastic selection is lower. It comes mainly from elastic Z production ($ep \to epZ^0$, $Z^0 \to \nu\bar{\nu}$) and from the $\gamma\gamma \to e^+e^-$ process. The main uncertainty on the background comes from the limited MC statistics for NC DIS and heavy quarks.

In the elastic $ep \to \tilde{e}\chi_1^0 p$ selection, 20 to 30% of the events have the elastically scattered proton detected by the Leading Proton Spectrometer (LPS). The proton momentum $\mathbf{p}'$ measured in the LPS can be used to reconstruct kinematical variables such as the center of mass energy $W_{\gamma e} = m_{\tilde{e}\chi_1^0}$ (fig. 5 a) and the missing mass $m^2_{\chi_1^0\chi_1^0} = (\mathbf{p} + \mathbf{e} - \mathbf{p}' - \mathbf{e}')^2$ (fig. 5 b), allowing a measurement of the mass of SUSY particles. Moreover the background from elastic Z0 events can be removed by a cut on $m_{\chi_1^0\chi_1^0}$.

4 Search Reach

Given an expected integrated luminosity L and assuming a number of detected events equal to the expected background $n_0 = \mu_B = bL$, a 90% CL upper limit on the signal events $N^{90\%}$ can be set [8]. This limit can be transformed in an exclusion plot on $m_{\tilde{e}}$ and $m_{\chi_1^0}$, excluding the mass sets that satisfy $\sigma(m_{\tilde{e}}, m_{\chi_1^0})\epsilon L > N^{90\%}$.

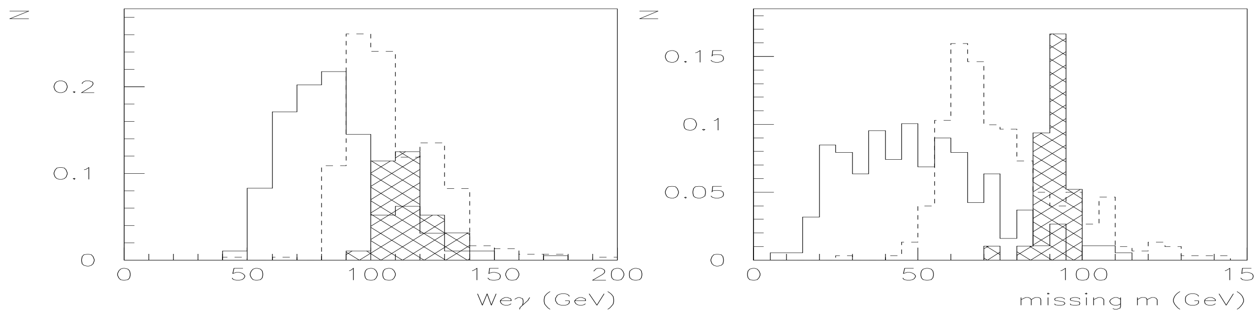

Figure 5: *Distributions of kinematical quantities reconstructed from the elastically scattered proton detected in the LPS. a) The center of mass $W_{\gamma e} = m_{\tilde{e}\chi_1^0}$ mass and b) the missing mass $m_{\chi_1^0\chi_1^0}$. The filled histogram is elastic Z0 background, the full line is $m_{\tilde{e}} = 40$, $m_{\chi_1^0} = 5$ and the dashed line is $m_{\tilde{e}} = 60$, $m_{\chi_1^0} = 25$. Note that $m_{\tilde{e}} + m_{\chi_1^0} = \min(W_{\gamma e})$ and $2m_{\chi_1^0} = \min(m_{\chi_1^0\chi_1^0})$*

Figure 6 a-b) shows the contours of the 90% CL excluded region for different luminosities for $\chi_1^0 = \tilde{\gamma}$ and $m_{\tilde{e}_R} = m_{\tilde{e}_L}$. Figure 6 c-d) shows the 90% CL excluded regions with a luminosity of 1000 pb^{-1} in the MSSM, assuming the relation $\frac{M_1}{M_2} = \frac{5}{3}\sin\theta_w$. Since the selectron can decay also to chargino and to the second neutralino, the branching ratio $\tilde{e} \to e\chi_1^0$ (evaluated with the ISASUSY[9] code) has been taken into account. The dash-dotted line is the limit for the process $e^-p \to \tilde{e}_R^-\chi_1^0X$, i.e. the case of the left handed selectron heavyer than right handed. The shaded area shows the region excluded by LEP1 and LEP1.5. [10]. The elastic selection is the more promising: with a luminosity $\sim 1fb^{-1}$ existing limits can be substantially improved.

Acknowledgments

I wish to thank R.Nania, M.Basile and I.Gialas for their unvaluable suggestions and A.Zichichi for having initiated and stimulated these studies.

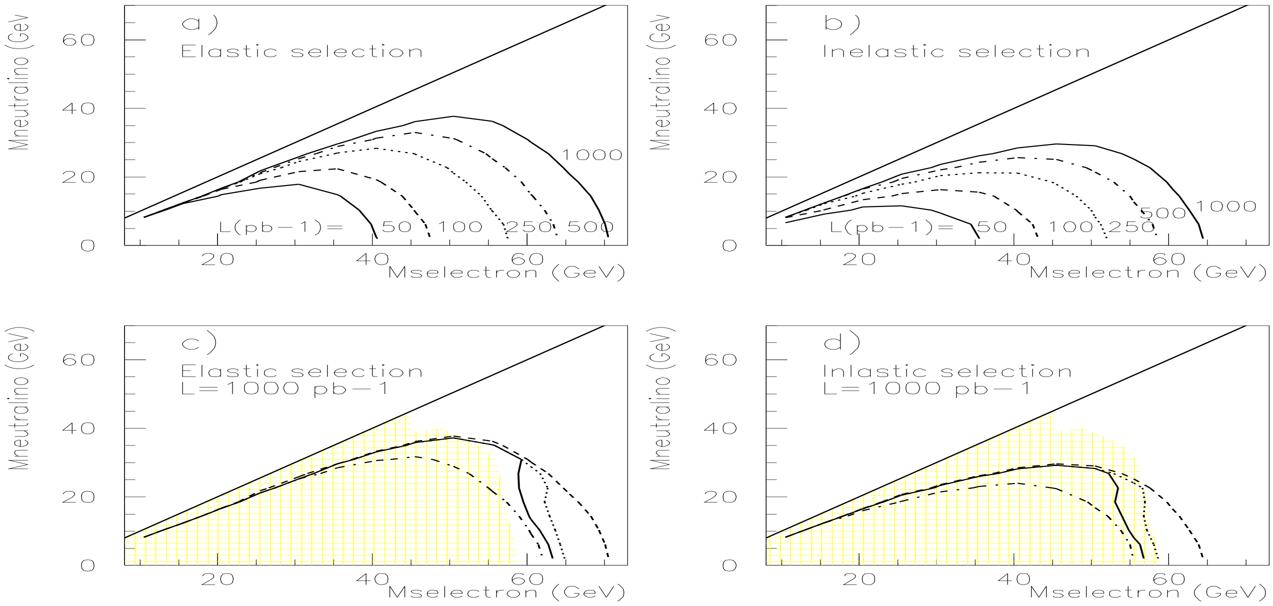

Figure 6: *Contours of the regions excluded at 90% CL in the plane* $m_{\chi_1^0}$ *vs* $m_{\tilde{e}}$ *for the elastic (a,c) and the inelastic (b,d) selection. a,b) for various values of the integrated luminosity in the pure photino case. c,d) for fixed luminosity (1 fb*$^{-1}$*) and different values of the MSSM parameters:* $\tan\beta = 1.41$, $\mu = -50$ *(dashed line);* $\tan\beta = 1.41$, $\mu = -500$ *(dotted line);* $\tan\beta = 35$, $\mu = -500$ *(solid line);* $m_{\tilde{e}_L} >> m_{\tilde{e}_R}$ *(dash-dotted line). The hatched area is excluded by LEP.*

References

[1] A.Lahanas and D.V.Nanopoulos, Phys Rep. 145(1987) 1 and references therein;

[2] J.L.Lopez, D.V.Nanopoulos and A.Zichichi, PRD 49(1994)343, Int. J. Mod. Phys. A 10(1995)4241, PRD 52(1995)4178, and PRD 53(1996)5253; J.Lopez and D.V.Nanopoulos, PRL 76(1996)1566, hep-ph/9412332 (int. J. Mod. Phys. A) , hep-ph/9607220; J.L.Lopez, D.V.Nanopoulos and K. Yuan, Nucl. Phys. B399(1993)654;

[3] J.Lopez *et al.* CERN-TH.7401/94;

[4] J.L.Lopez, D.V.Nanopoulos, X. Wang and A.Zichichi, PRD 48(1993)4029.

[5] P.Salati, J.Wallet PLB 122(1983)397; G.Altarelli, *et al.* Nucl. Phys. B262(1985)204; M.Drees, D.Zeppenfeld PRD 39(1989)2536;

[6] H.Tsutsui *et al.* PLB245(1990)663;

[7] B.A.Kniehl PLB 254(1991)267;

[8] L.Montanet *et al.* (PDG) Review of Particle Properties, PRD 54(1996) equation 28.40;

[9] H.Baer *et al.* in *Physics at Current Accelerators and Supercolliders*, J. Hewett *et al.* editors, (Argonne N.L. 1993);

[10] Decamp *et al.* (ALEPH coll.) Phys.Rep. 216(1992)253; Adriani *et al.* (L3 coll.) Phys.Rep. 236(1993)1; ALEPH coll. CERN PPE 96-10;